High-temperature and "exotic" minerals from the Cioclovina Cave, Romania: a review

Bogdan P. ONAC[1,2] *, Herta S. EFFENBERGER[3] & Radu C. BREBAN[4]

[1] Department of Geology, University of South Florida, 4202 E. Fowler Ave., SCA 528, Tampa, FL 33620, USA
[2] Department of Mineralogy, „Babeș-Bolyai" University, Kogălniceanu 1, 400084 Cluj Napoca, Romania
„Emil Racoviță" Institute of Speleology, Clinicilor 5, 400006 Cluj Napoca, Romania
[3] Institut für Mineralogie und Kristallographie, Universität Wien, Althanstraße 14, 1090 Wien, Austria
[4] SpeleoClub "Proteus", Aleea Pescarilor, Bl. 30/47, Deva, Hunedoara, Romania

ABSTRACT. This paper reports on the identification of four rare minerals in the phosphate deposit in Cioclovina Cave, Romania. Berlinite, $AlPO_4$ and hydroxylellestadite, $Ca_5[(Si,P,S)O_4]_3(OH,F,Cl)$ are minerals that can form only at high temperatures, and would not be expected in a sedimentary environment. In this study we review the characteristics of berlinite and hydroxylellestadite from a heated sedimentary sequence in Cioclovina Cave (Romania) and refine their structure from single-crystal X-ray data. Two other minerals, churchite-(Y), $YPO_4·2H_2O$ and foggite, $CaAl(PO_4)(OH)_2·H_2O$ are, for the first time, described from a cave environment. The minerals were documented by means of single-crystal X-ray investigations, X-ray powder diffraction, and electron-microprobe (EMPA) analyses. In addition, laboratory synthesis of berlinite was conducted and vibrational spectroscopy data were collected for hydroxylellestadite and churchite-(Y). Based on these investigations, we suggest that locally the heavily compacted phosphate-bearing clay sediments underwent a natural heating process. It is likely that in-situ bat guano combustion is responsible for generating the high-temperature environment needed for the genesis of berlinite and hydroxylellestadite. The occurrence of churchite-(Y) and foggite is related to guano-leaches that reacted with subjacent limestone and different allogenic cave sediments.

Key words: cave minerals, guano combustion, Cioclovina Cave, Romania.

INTRODUCTION

Over 275 minerals are precipitated within the cave environments when solutions of various origin and chemical composition react with different cave deposits (i.e., speleothems, terrigenous sediments or organic detritus) (Hill and Forti, 1997; Onac, 2005). Of great interest are those minerals identified in particular cave environments (skarn-hosted caves, cavities carved by H_2S-rich or hydrothermal ore-forming solutions, lava tubes, etc.), because they precipitated under highly unusual conditions that are not common for the majority of caves. Caves containing large amounts of bat guano also fall within this category for two main reasons: (1) percolating water passing through guano enriches in phosphate and upon its reaction with limestone or other detrital sediments is precipitating some rare minerals; (2) spontaneous combustion of bat guano (Oakley, 1954) may locally cause thermal transformation of the surrounding cave sediments, hence generating unusual high-temperature minerals.

A number of studies have shown that these two processes are responsible for the occurrence of at least 20 rare minerals (Martini, 1994a, b; Urbani, 1996; Hill and Forti, 1997 and citations therein; Martini, 1997; Onac et al., 2002, 2005, 2006; Onac and White, 2003; Forti, 2005; Onac and Effenberger, 2007).

This paper reviews the most unusual minerals reported to date from Cioclovina Cave (Șureanu Mountains, Romania). Over the last five years, we have thoroughly documented four minerals out of 27 known in this cave (Onac et al., 2005, 2006; Onac and White, 2003; Onac and Effenberger, 2007). Five other minerals (crandallite, tinsleyite, leucophosphite, taranakite, and brushite) were characterized in detail by Constantinescu et al. (1999), Dumitraș and Marincea (2000), Dumitraș et al. (2004), Marincea et al. (2002), and Marincea and Dumitraș (2003). These later minerals, as well as a number of other rarities (e.g., burbankite, collinsite, sampleite) that are still in the process of single-crystal X-ray investigations are not included in this review.

## CAVE DESCRIPTION AND MINERAL OCCURRENCE

Cioclovina Cave is one of the most important caves within the Șureanu Mountains (Romania), both in terms of length and scientific interest. It is well documented that Cioclovina Cave hosts important archeological, anthropological, and paleontological remains (Breuil, 1925; Roska, 1925; Simionescu, 1941; Banerjee et al., 1999; Păunescu, 2001; Olariu et al., 2002; Breban et al., 2003)

*Correspondence: B.P. Onac (bonac@cas.usf.edu)

along with an impressive collection of rare minerals (Onac, 2003). In order to preserve such a complex scientific archive, the cave was included within the Grădiştea Muncelului – Cioclovina Natural Park.

The Ponorici-Cioclovina cu Apa (Wet Cioclovina) cave system is located in the southwestern side of the Şureanu Mountains, 34 km east of the city of Hunedoara.

The cave is formed in a 350-m thick sequence of Upper Jurassic and Lower Cretaceous limestones and consists of 4,272 m of passages (Fig. 1). The minerals presented in this review were collected from various outcrops scattered along ~450 m of galleries located in the vicinity of the natural entrance in the Cioclovina Uscată (Dry Cioclovina) Cave.
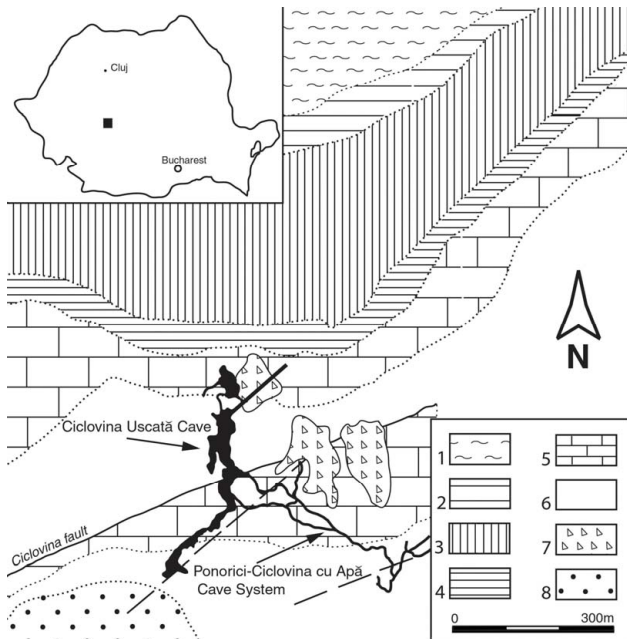
Fig. 1. *Location map of the study site in central-western part of Romania. Plan map of Cioclovina Cave and the surrounding geology; 1: Precambrian schists & gneisses; 2: Cioclovina Red Bed (Lower Permian); 3: Lower Jurassic conglomerates & sandstones; 4: Limy sandstone (mid-Jurassic); 5: Cherty limestone (Upper Jurassic); 6: Reef limestone (Lower Cretaceous); 7: Quaternary sediments; 8: Upper Cretaceous sandstones & marls (geology after Stillă, 1981).*

Before describing the occurrence of minerals, a brief overview of the sedimentological setting of the cave is provided. Initially, the cave was almost completely filled with clastic sediments (clay, sand, and gravel), which contain interbedded layers of organic material (bat guano and/or bone breccia). Due to the high content in P_2O_5 (up to 30% wt) of these sediments, extensive mining of the phosphates sediments was undertaken over three distinct time intervals (1912-1918, 1923-1928, and 1938-1941). A major consequence of mining is that several good sediment exposures are now available throughout the lower part of the cave (Fig. 2a).

The clastic sediments exposed between the cave entrance and the middle parts of the Bivouac Room are typical alluvial deposits of various grain sizes. In a restricted section of the Bivouac Room, the overburden sediment was so significant that the underlying material was so heavily compacted that textures and structures of the original sediments can no longer be recognized (Fig. 2b). In this part of the cave, owing to microbial processes, the temperature inside the buried guano increased until spontaneous ignition

led to its combustion, converting the sediment to a dark brown color. This thermal process further obliterated the outlines of the original depositional features.


Fig. 2. *a) Outcrop of fluvial sediments unaffected by guano combustion; b) Vein of thermally-transformed sediments in the Bivouac Room.*

Berlinite appears as colorless, sometimes grayish sub-millimeter well-crystallized aggregates, chaotically disposed within the heavily compacted magenta to dark brown-colored phosphate-rich sediments (Fig. 3a). Visually, the berlinite crystals are not distinguishable from quartz, hence they are easily overlooked (Onac and White, 2003; Onac and Effenberger, 2007).

Hydroxylellestadite occurs as light-orange xenomorphic crystals associated with quartz (Fig. 3b). The aggregate grain size is up to 1.5 mm in length and 0.3 mm across (Onac et al., 2006). The berlinite and hydroxylellestadite-bearing sediment occurs only in a dead-end, side passage of the Bivouac Room and shows all compaction and thermal transformation features just described.

White-pinkish to gray (sometimes even black) crusts and earthy-masses of ***foggite*** (Fig. 3c) were collected from a sandwiched sequence of crusts, just below a reddish -brown crandallite-rich clay horizon in the so-called Sala Septei (Pendant Room) (Onac et al., 2005). Similar material was observed and identified as foggite near the entrance into the Bivouac Room.

Churchite-(Y) occurs in a few sections near the entrance into the Bivouac Room. Under the stereomicroscope, the crystals show radiating acicular habit. The largest crystals are up to 0.6 mm in length (Fig. 3d). In most of the occurrences, churchite-(Y) was intimately associated with brushite. Churchite-(Y) crystals have a vitreous luster and are translucent (Onac et al., 2005). Scanning electron micro-photographs also revealed platy crystals of churchite-(Y) (Onac et al., 2002).
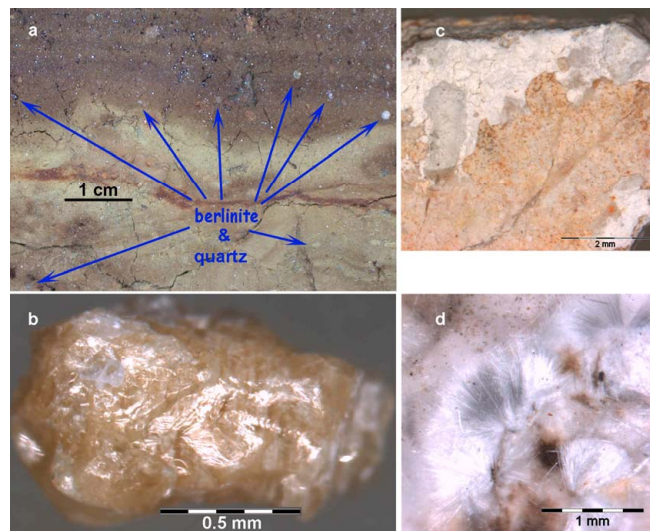
Fig. 3. *a) Berlinite and quartz grains in sediments affected by guano fire; b) Grain of hydroxylellestadite; c) Crust of foggite; d) Needle-like crystals of churchite-(Y).*

METHODS AND INSTRUMENTATION

Visual inspection of all specimens was undertaken with a NIKON Optiphot2-POL and an Olympus SZX12 stereo-microscope at magnifications ranging from 10 to 63x.

The chemical analyses were performed in energy- and wavelength-dispersion mode using a Jeol JSM-6310 instrument with attached EDX Oxford Link Isis and Microspec WDX (analytical conditions: 15 kV, 5 and 10 nA, 1.5 to 3 m beam size, WDX: peak count-time 20 s, background count-time 10 s). A 100-s real-time scan in EDS mode revealed F, Si, P, S, Cl, and Ca. No other elements with Z greater than 8 were found. The Phi-Rho-Z program incorporated in the ISIS software was used for data reduction. Apatite (Ca, F), quartz (Si), xenotime (P), celestine (S), and atacamite (Cl) served as standards for hydroxylellestadite. For churchite-(Y) and foggite, the probe standards were synthetic corundum (Al), quartz (Si), adularia (K), apatite and calcite (P and Ca), garnet (Fe), synthetic YPO_4 (P and Y), and REE-fluorides GdF_3, DyF_3, ErF_3, YbF_3 (Gd, Dy, Er, Yb).

Except for the standards, an additional microprobe analysis on the new available berlinite material was performed using the analytical protocol described in Onac and White (2003). Natural garnet was used for Al, Fe, and Si, whereas fluorapatite replaced variscite for P.

Small crystal chips of berlinite and hydroxylellestadite were examined with a Nonius Kappa-CCD four-circle diffractometer equipped with a 300 μm diameter capillary-optics collimator (graphite-monochromatized MoK_α radiation). Data were corrected for background, Lorentz and polarization effects, and absorption (multi-scan method).

Programs used include COLLECT (Nonius, 1999), DENZO-SMN (Otwinowski and Minor, 1997), and SHELXL-97 (Sheldrick, 1997).

X-ray powder diffraction patterns for both foggite and churchite were collected with a Siemens D5000 Kristalloflex (Bruker AXS, twin Goebel mirrors) and Bruker AXS D8 Advance diffractometers using Cu-K_α radiation (kV = 40; mA = 40; step 0.040°; step time 2 s). The calibration standard was quartz.

The FT-IR spectra of hydroxylellestadite and churchite-(Y) (KBr pellet) were recorded at room temperature using a Bruker Equinox 55 spectrometer (InGaAs detector) and a Perkin-Elmer 1760X FT-IR spectrometer (NIR spectral range, 400 – 4000 cm^{-1}) at the "Babeş-Bolyai" University in Cluj. Two hundred scans were accumulated, all with a spectral resolution of 4 cm^{-1}. In addition, micro-Raman spectra of two different hydroxylellestadite samples were taken with a Dilor Labram spectrometer (514.5 nm excitation line) from a 100 mW Spectra Physics Argon ion laser (back-scattering geometry) at the University of Wuerzburg, Germany.

All mineralogical and crystallographic investigations reported in the present paper were conducted at the Institute of Mineralogy and Petrology, Karl-Franzens University in Graz and at the Institute of Mineralogy and Crystallography, University of Vienna, Austria.

HIGH-TEMPERATURE MINERALS

Berlinite

The single-crystal X-ray refinement converged at $R1(F) = 0.0276$, $wR2(F^2) = 0.0657$ for 677 reflections ($2\theta_{MoK\alpha} \leq 70°$) and 31 variables in space-group $P3_121$ ($a = 4.946(1)$, $c = 10.953(2)$ Å, $V = 232.0$ Å^3, $Z = 3\{AlPO_4\}$) (Table 1). The average $<T—O>$ bond distances within the two crystallographically different TO_4 tetrahedra are 1.734 and 1.526 Å, respectively (Table 2).

From the scattering power at these T sites and the stereochemistry, the presence of an AlO_4 beside a PO_4 tetrahedron is doubtless. Consequently, the sample from Cioclovina Cave is verified as $AlPO_4$ (modification berlinite). The features of the crystal structure determined during this work agree with those found by Sowa et al. (1990) and Muraoka and Kihara (1997) for synthetic $AlPO_4$ samples under ambient conditions (see also Cora et al., 2003). Furthermore, the determination of the unit-cell metrics showed that the sample definitely is not quartz as suggested by Marincea and Dumitraş (2005). The a cell parameter is somewhat larger than expected for low-quartz and c cell parameter is doubled.

The electron-microprobe analyses published by Onac and White (2003) gave a total of 99.96 and 99.68 wt%, respectively. The analytical formula reported was $Al_{0.993}P_{0.998}O_4$, consistent with the expectations for berlinite. To confirm our findings we have performed an additional microprobe analysis on the new available material, using the analytical protocol described in Onac and White (2003), but with a new set of standards (natural garnet for Al, Fe, and Si, and fluorapatite for P). The mean of five analyses (total = 99.99 wt%) on a single berlinite grain yielded the chemical formula: $Al_{0.998}(P_{1.002}Si_{0.001})_{\Sigma=1.003}O_4$ (normalized on the basis of 4 O atoms per formula unit) confirming the presence of berlinite.

Table 1. *Single-crystal X-ray data collection and structure refinement for berlinite.*

a (Å)	4.946(1)
c (Å)	10.953(2)
V (Å³)	232.0
Space group	$P3_121$
Z	3 {AlPO$_4$}
Crystal diameter (mm³)	$0.025 \times 0.042 \times 0.17$
Absorption coefficient μ (mm^{-1})	0.99
Scan range $\Delta\varphi$ (at 11 distinct ω values) (°)	2
Collection time (s/°)	140
$2\theta_{max}$ (°)	70
Number of images measured	561
Crystal-detector distance (mm)	30
Data collection temperature (K)	293
Measured / unique reflections (n)	3996 / 677
$R_{int} = \Sigma \|F_o^2 - F_o^2(\text{mean})\| / \Sigma F_o^2$	0.0276
$R1(F) / wR2(F^2)^*$ (for the 677 unique reflections)	0.0276 / 0.0657
$R1(F)$ (for the 629 reflections with $F_o > 4\sigma(F_o)$)	0.0246
Variable parameters (p)	31
GooF = $\{\Sigma [w(F_o^2 - F_c^2)^2] / (n-p)\}^{0.5}$	1.065
Δ/σ	< 0.001
$\Delta\rho_{min}, \Delta\rho_{max}$ (eÅ^{-3})	-0.33, 0.37
Extinction coefficient	0.098(15)
$R1(F) = \Sigma(\| \|F_o\| - \|F_c\| \|) / \Sigma F_o; wR2(F^2) = [\Sigma w(F_o^2 - F_c^2)^2 / \Sigma w F_o^4]^{1/2}$	
$w = 1 / \{\sigma^2(F_o^2) + [0.044*[\max(0,F_o^2) + 2*F_c^2) / 3]]^2 \}$	

Table 2. *Bond distances (Å) for berlinite.*

Al—O1^{0,ii}	1.7301(10)	P—O1$^{i, iv}$	1.5270(9)
Al—O2$^{i, v}$	1.7381(10)	P—O2$^{0, iii}$	1.5242(11)
O1^0—Al—O1^{ii}	111.72(8)	O1^i—P—O1^{iv}	108.82(8)
O1^0—Al—O2^i	107.29(3)	O1^i—P—O2^0	109.08(4)
O1^0—Al—O2^v	109.45(5)	O1^i—P—O2^{iii}	110.83(6)
O1^{ii}—Al—O2^i	109.45(5)	O1^{iv}—P—O2^0	110.83(6)
O1^{ii}—Al—O2^v	107.29(3)	O1^{iv}—P—O2^{iii}	109.08(4)
O2^i—Al—O2^v	111.70(8)	O2^0—P—O2^{iii}	108.20(8)

Symmetry code: ^{0} x, y, z; ^{i} $-x+1, -x+y, -z+4/3$; ^{ii} $x-y, -y, -z+2/3$; ^{iii} $x-y, -y, -z+5/3$; ^{iv} $-y+1, x+y, z+1/3$; ^{v} $-y+1, -x-y, z-2/3$.

Hydroxylellestadite

The mean of eight electron-microprobe analyses of hydroxylellestadite yielded the empirical formula $Ca_{10.27}[(SiO_4)_{2.53}(SO_4)_{2.17}(PO_4)_{1.27}]_{\Sigma=5.97}[(OH)_{1.66}F_{0.21}Cl_{0.16}]_{\Sigma=2.03}$ (the cations are normalized to neutralize 26 oxygen-equivalents (i.e., 24 O atoms and 2 (OH + F + Cl); see Table 3).

Water was not determined experimentally but recalculated for charge balance of the chemical formula. A micro-chemical test for carbonate by evaporating CO_2 was negative. The composition of hydroxylellestadite is quite homogeneous, both within a given crystal as well as between different samples. The strong depletion in Cl and F counterbalanced by enrichment of OH shifts the anion composition to a nearly pure end-member hydroxyl-ellestadite.

The presence of a large S component (16.85 wt% SO$_3$), coupled with excess Si (14.73 wt% SiO$_2$) not balanced by the $(CO_3)^{2-}$ or (Y + rare earth element (*REE*)), implies the existence of an isomorphous charge-compensated substitution, namely: $2P^{5+} \leftrightarrows Si^{4+} + S^{6+}$, as proposed by McConnell (1937).

An X-ray single-crystal-structure investigation gave the average space-group symmetry $P6_3/m$ ($R1(F) = 0.038$ for 783 reflections up to $2\theta_{MoK\alpha} = 70°$ and 42 variables, $a = 9.496(2)$, $c = 6.920(2)$ Å, $V = 540.4$ Å^3, and $Z = 2$, confirming the presence of hydroxylellestadite (Table 4). For further information on hydroxylellestadite structure refinement see Onac et al. (2006).

Table 3. *Electron-microprobe analyses of hydroxylellestadite.*

wt%	Mean of 8 analyses	Range	Number of ions	
SiO$_2$	14.73	14.54-14.94	Si	2.53
P$_2$O$_5$	8.73	8.45-8.92	P	1.27
SO$_3$	16.85	16.53-17.09	S	2.17
CaO	55.84	54.92-56.93	Ca	10.27
F	0.39	0.36-0.43	F	0.21
Cl	0.54	0.49-0.56	Cl	0.16
H$_2$O	1.45	-	-	-
OH	-	-		1.90
-O=(F,Cl)	0.29	-	-	-
Total	98.24	-	-	-

The overall vibrational analyses of our samples show significant phosphate modes contribution, characteristic for an apatite with a partial substitution of $(PO_4)^{3-}$ ions by $(SO_4)^{2-}$ and $(SiO_4)^{4-}$. The large band centered at 928 cm^{-1} with a shoulder at 853 cm^{-1} is characteristic for the SiO$_4^{4-}$ group.

The shifts however, observed between our vibrational frequencies and those reported by Harada et al. (1971), Arkhipenko and Moroz (1997), and Socrates (2001) reflect the partial substitution of $(SiO_4)^{4-}$ and $(SO_4)^{2-}$ for the $(PO_4)^{3-}$ group in the apatite structure. Based on Santos and Clayton (1995) and Popović et al. (2005), the IR bands at 1144 and 1049 cm^{-1} from our spectrum were assigned to either double or single bond stretching of an orthophosphate and not to the $(SO_4)^{2-}$ group as suggested by Harada et al. (1971) and Sejkora et al. (1999).

Therefore, the most obvious difference, when compared to the previously reported data, was found in the increasing relative intensity of the $(PO_4)^{3-}$ lines.

Table 4. *Single-crystal X-ray data collection and structure refinement for hydroxylellestadite.*

a (Å), c (Å); V (Å³); space group	9.496(2), 6.920(2); 540.4; $P6_3/m$
Z	2 $\{Ca_5[(Si,P,S)O_4]_3(OH,F,Cl\}$
Crystal diameter (mm³); μ (mm⁻¹)	$0.045 \times 0.050 \times 0.065$; 3.0
Δφ at 12 distinct ω values (°); collection time (s/°)	2; 110
$2\theta_{max}$ (°); images; crystal-detector distance (mm)	70; 723; 30
Data collection temperature (K)	293
Measured reflections; $R_{int} = \Sigma \|F_o^2 - F_o^2(mean)\| / \Sigma F_o^2$	9429; 0.043
Unique (n) reflections; $R1(F)$; $wR2(F^2)^*$,	845; 0.041; 0.090
'Observed' reflections $F_o > 4\sigma(F_o)$; $R1(F)$	783; 0.038
GooF = $\{\Sigma[w(F_o^2 - F_c^2)^2] / (n-p)\}^{0.5}$	1.059
Variable parameters (p); Δ/σ; $\Delta\rho_{min}$, $\Delta\rho_{max}$ (e/Å³)	42; < 0.001; -1.33, 1.77
Extinction coefficient	0.012(3)

$R1(F) = \Sigma(\|\,|F_o| - |F_c|\,\|) / \Sigma F_o$; $wR2(F^2) = [\Sigma w(F_o^2 - F_c^2)^2 / \Sigma wF_o^4]^{1/2}$

$w = 1 / \{\sigma^2(F_o^2) + [0.033*P]^2 + [1.37*P]\}$, P = $[max(0,F_o^2)] + 2*F_c^2] / 3$

"EXOTIC" MINERALS

Foggite

The X-ray powder pattern of foggite crust is reported in Table 5. Least square refinement of unit-cell parameters using 19 reflections ($12° < \theta < 55°$) gave: $a = 9.271(3)$ Å, $b = 21.324(3)$ Å, $c = 5.1906(2)$ Å, and $V = 1026.188(2)$ Å³ ($Z = 4$) which are in good agreement with those reported by Moore et al. (1975).

The mean of nine point electron microprobe analyses within one polished thin section (Table 6) yields the following empirical formula:
$Ca_{0.925}(Al_{0.91}Fe^{2+}_{0.016})_{\Sigma=0.926}(P_{0.991}Si_{0.043})_{\Sigma=1.03}O_{3.74}(OH)_{2.26}\cdot H_2O$, based on (O+OH) = 7, which may be written in simplified form as: $CaAl(PO_4)(OH)_{2.26}\cdot H_2O$. Foggite is inhomogeneous on a micrometer scale (see Table 6), all chemical compounds varying within ~2 wt%.

Backscattered electron images show three distinct horizons (each of different gray shades). Our microprobe analyses indicate the upper dark gray sector corresponds to a crandallite composition, the gray material located in the middle section is foggite, whereas the gray light-gray horizon underlying foggite appears to be Ca-depleted foggite (P_2O_5 = 35.66 and CaO = 10.34 wt%). Locally, within the later unit the composition corresponds to that of variscite (P_2O_5 = 47.30 and Al_2O_3 = 30.47 wt%).

Churchite-(Y)

The chemical composition of churchite is variable from grain to grain, but each grain is homogeneous. Apart from Y, which is the main chemical element, variable amounts of rare-earth-elements (REEs) were observed. Most of the grains contain up to 4.02 wt% dysprosium (Dy) and 3.35 wt% Er. In addition, gadolinium (Gd), ytterbium (Yb), and traces of Ca (up to 0.26 wt%) have been identified.

All of the chemical analyses show Dy > (other REEs) that argues for a Dy-rich churchite-(Y) in Cioclovina Cave. The mean Y: (Gd,Er,Dy,Yb) ratio was found to be 4:1. The average of 11 analyses (each with 2 or 3 repetitions) is given in Table 6. A defocused beam was used in order to avoid sample deterioration, hence this effect is judged insignificant. The empirical formula calculated for O = 4 is:

$[Y_{0.819}(Dy_{0.042}Er_{0.031}Gd_{0.028}Yb_{0.021})_{\Sigma=0.122}Ca_{0.009}]P_{1.01}O_{4.00}\cdot 2.09H_2O$, which corresponds well to an ideal formula $(Y+REE)PO_4\cdot 2H_2O$.

The results of the X-ray powder diffraction are compiled in Table 5. Unit-cell dimensions of monoclinic Dy-rich churchite, refined from 38 unambiguously indexed reflections ($10° < \theta < 70°$) using the program of Holland and Redfern (1997) are $a = 5.611(5)$ Å, $b = 15.045(2)$ Å, $c = 6.196(1)$ Å, b = 115.86(2)°, and $V = 470.714(4)$ Å³ ($Z = 4$).

The unit-cell is much closer to the Cornwall churchite described by Claringbull and Hey (1953) and quite different from the Auerbach churchite-(Y) (Kohlmann et al., 1994). The observed differences between the cell units might be due to substitutions of larger REE ions for Y.

The vibrational spectra of hydrated rare earth phosphates, in particular those of churchite are sparse (Petruševski and Šoptrajanov, 1984; Assaaoudi and Ennaciri, 1997; Assaaoudi et al., 2001; Lucas et al., 2004). The FTIR spectrum obtained exhibits all the bands assigned to the vibrations of PO_4 and the specific bands of O-H and H-O-H.

The small shifts observed between our vibrational frequencies and those reported by Assaaoudi and Ennaciri (1997) might be attributed to partial replacement of Y by lanthanide cations of larger ionic radius (Onac et al., 2005).

CONCLUDING REMARKS

To form berlinite and hydroxylellestadite in a cave environment, two major requirements need to be satisfied: the appropriate chemical ingredients and the heating source must be available. The presences of the two minerals are strong indicators that the heavily compacted phosphate-bearing clay sediments underwent a natural heating process probably caused by in-situ guano combustion. It is difficult to imagine any other process able to generate the required-temperature (above 550 ºC) within the cave environment.

With respect to the chemical ingredients, a number of minerals known to occur in Cioclovina Cave could have acted as starting material.

In particular, taranakite, tinsleyite, and crandallite (Constantinescu et al., 1999; Marincea et al., 2002), might have been sources for berlinite.

Table 5. *X-ray powder diffraction data for foggite and churchite-(Y).*
Indexing and d_{ref} based on the atomic arrangement of foggite (Moore et al., 1975) and churchite-(Y) (Kohlmann et al., 1994)
program LAZY PULVERIX (Yvon et al., 1977).

	Foggite					Churchite-(Y)			
hkl	d_{obs} (Å)	d_{calc} (Å)	I_{hkl}	d_{ref} (Å)	hkl	d_{obs} (Å)	d_{calc} (Å)	I_{hkl}	d_{ref} (Å)
020	10.667	10.665	3	10.662	020	7.516	7.508	100	7.503
120	6.989	6.993	13	6.994	011	5.199	5.197	46	5.205
220	4.249	4.248	100	4.249	121	4.191	4.181	39	4.180
031	4.192	4.195	39	4.202	040	3.751	3.754	18	3.752
131	3.823	3.821	24	3.827	141	3.001	3.009	39	3.008
240	3.497	3.496	17	3.497	022	2.597	2.598	5	2.602
151	3.105	3.106	46	3.109	060	2.500	2.502	7	2.501
320	2.966	2.965	15	2.967	222	2.382	2.386	4	2.386
251	2.685	2.686	51	2.688	152	2.159	2.163	5	2.163
080	2.665	2.666	17	2.665	242	2.087	2.090	3	2.090
102	2.499	2.501	11	2.507	240	2.056	2.057	27	2.061
271	2.285	2.286	23	2.287	112	2.017	2.020	24	2.026
411	2.106	2.104	5	2.106	170	1.963	1.966	6	1.966
191	2.098	2.100	9	2.101	080	1.872	1.877	4	1.876
1 11 1	1.782	1.782	8	1.783	062	1.853	1.857	4	1.858
391	1.768	1.767	5	1.768	143	1.820	1.818	3	1.819
3 10 0	1.755	1.755	8	1.755	262, 321	1.771	1.774	8	1.774
480	1.749	1.750	13	1.749	260	1.754	1.754	6	1.756
471	1.737	1.737	8	1.738	323	1.636	1.637	3	1.638
402	1.734	1.728	14	1.731	181, 091	1.593	1.597	3	1.597
282	1.728	1.726	13	1.728	204	1.558	1.559	20	1.560
531	1.695	1.694	5	1.696	224	1.527	1.526	2	1.527
					202	1.522	1.519	3	1.524
					282	1.504	1.504	3	1.504
					0 10 0	1.499	1.501	1	1.501
					134	1.466	1.466	1	1.468
					314	1.436	1.436	3	1.437
					143	1.406	1.401	12	1.405
					402	1.394	1.392	3	1.394
					1 10 1	1.346	1.346	3	1.346
					383, 0 12 0	1.249	1.251	3	1.251

Table 6. *Microprobe data of foggite and churchite.*

Foggite	Mean (n = 9) [wt%]	Range	Cations based on: 7(O+OH)	Ideal (%)
Al_2O_3	21.788	21.09 – 22.34	0.91	23.82
P_2O_5	33.045	31.98 – 33.99	0.991	33.16
CaO	24.36	23.42 – 24.85	0.925	26.20
SiO_2	1.232	0.59 – 2.23	0.043	-
FeO	0.521	0.32 – 1.05	0.016	-
H_2O	18.04	-	7.25	16.83
Total	98.986	-	-	100.00
Churchite	(n = 11)		4O (x 1.5)	
Y_2O_3	40.414	36.07 – 45.3	0.819	51.34
P_2O_5	31.325	27.93 – 36.03	1.01	32.27
Gd_2O_3	2.245	2.06 – 2.41	0.028	-
Dy_2O_3	3.431	3.13 – 4.02	0.042	-
Er_2O_3	2.698	2.50 – 3.35	0.032	-
Yb_2O_3	1.833	1.58 – 2.13	0.021	-
CaO	0.225	0.19 – 0.26	0.012	-
H_2O	16.12	-	4.098	16.38
Total	98.291	-	-	99.99

These minerals, along with ardealite, brushite, carbonate-hydroxylapatite, hydroxylapatite, and monetite (all derived from bat guano) explain our PO_4-rich hydroxylellestadite. The sulfate in this later mineral likely originated from gypsum and/or ardealite (both minerals are abundant in the cave), whereas silica is thought to be contributed by the clastic sediments (sand and clay) that cover the guano deposits. Calcium comes from limestone and secondary cave calcite deposits. Either a calcium phosphate apatite (in the presence of sulfate and silica) or a mixture of the above ingredients could have been transformed into hydroxylellestadite if spontaneous combustion of bat guano occurred locally within the cave.

The remarkable new occurrence of foggite and churchite reported from Cioclovina Cave, Romania, provides a sharp contrast to the other previously documented localities, all related to somehow different environments (i.e., pegmatites, weathered profiles, laterites, and bauxites) (Onac et al., 2005). Foggite was likely formed at the expense of the originally precipitated crandallite. Our backscattered images and electron microprobe investigation support this hypothesis (i.e., the foggite horizon was always identified below a crandallite-rich layer) and suggests a progressive transformation of crandallite into foggite as the percolating solutions become depleted with respect to Al_2O_3 and P_2O_5 while descending through the thick floor-accumulated clay-rich cave sediments.

With respect to churchite-(Y) origin, three possible sources for Y and REEs are to be considered: 1) they occur in trace amounts in most of the rocks; 2) weathering profiles are sometimes enriched in these elements, and 3) Y and REEs are omnipresent in soils, although in very small concentrations (Jones et al., 1996). Whatever the primary source of these elements is, percolating meteoric waters passing through the guano blanket, would mobilize the phosphates within. These mobile phosphates combined with Y- and REE-enriched cave sediments to precipitate churchite-(Y). The fact that only heavy REEs appear in churchite, suggests that during migration the solution would preferentially loose light REEs of whose stability is known to be lower than that of the heavy REEs (Millero, 1992; Henderson, 1996).

REFERENCES

Arkhipenko, D.K., Moroz, T.N. 1997, Vibrational spectrum of natural ellestadite. *Crystallography Reports*, 42: 651-656.

Assaaoudi, H., Ennaciri, A. 1997, Vibrational spectra and structure of rare earth orthophosphates, weinschenkite type. *Spectrochimica Acta*, 53A: 895–902.

Assaaoudi, H., Ennaciri, A. & Rulmont, A. 2001, Vibrational spectra of hydrated rare earth ortho-phosphates. *Vibrational Spectroscopy*, 25: 81–90.

Banerjee, A., Ghiurcă, V., Langer, B. & Manfred, W. 1999, Determination of the provenance of two archeological amber from Romania by FTIR and Solid-State-Carbon-13 NMR spectroscopy. *Archäologisches Korrespondenzblatt*, 29: 593-605.

Breban, R., Şerban, M., Viehmann, I. & Băicoană, M. 2003, *The history of guano-phosphate exploitation and the discovery of the human skull in the Ciclovina Uscata Cave (Hunedoara)*. Clubul de Speologie Proteus, Hunedoara, 138 p. (in Romanian with English abstract).

Breuil, H.A. 1925, Stations paleolithiques en Transylvanie. *Buletinul Societăţii de Ştiinţe din Cluj*, Tome II (4): 193-217.

Claringbull, G.F., Hey, M.H. 1953, A re-examination of churchite. *Mineralogical Magazine*, 223: 211-217.

Constantinescu, E., Marincea, Ş. & Crăciun, C. 1999, Crandallite in the phosphate association from Cioclovina cave, (Şureanu Mts., Romania). In: *Mineralogy in the system of the earth sciences* (Anastasiu, N., Ilinca, G., Eds). Imperial College Press, London, p. 1-5.

Cora, F., Alfredsson, M., Barker, C.M., Bell, R.G., Foster, M.D., Saadoune, I., Simperler, A. & Catlow, C.R.A. 2003, Modeling the framework stability and catalytic activity of pure and transition metal-doped zeotypes. *Journal of Solid State Chemistry*, 176 (2): 496-529.

Dumitraş, D.-G., Marincea, Ş. 2000, Phosphates in the bat guano deposit from the "Dry" Cioclovina Cave, Şureanu Mountains, Romania. *Romanian Journal of Mineral Deposits*, 79: 43-45.

Dumitraş, D.-G., Marincea, Ş. & Fransolet, A.M. 2004, Brushite in the bat guano deposit from the "dry" Cioclovina Cave (Şureanu Mountains, Romania). *Neues Jahrbuch für Mineralogie, Abhanflungen*, 180: 45-64.

Forti, P. 2005, Genetic processes of cave minerals in volcanic environments: an overview. *Journal of Cave and Karst Studies*, 67: 3-13.

Harada, K., Nagashima, K., Nakao, K. & Kato, A. 1971, Hydroxylellestadite, a new apatite from Chichibu mine, Saitama prefecture, Japan. *American Mineralogist*, 56: 1507-1518.

Henderson, P. 1996, The rare earth elements: introduction and review. In *Rare earth minerals. Chemistry, origin and ore deposits* (Jones, A.P., Wall, F. & Williams, C.T., Eds.), Chapman & Hall, London, p. 1-19.

Hill, C.A., Forti, P. 1997, *Cave minerals of the world* (2nd ed.). National Speleological Society, Huntsville, Alabama, 464 p.

Holland, T.J.B., Redfern, S.A.T. 1997, Unit cell refinement from powder diffraction data: the use of regression diagnostics. *Mineralogical Magazine*, 61: 65-77.

Jones, A.P., Wall, F. & Williams, C.T. (Eds.) 1996, *Rare earth minerals. Chemistry, origin and ore deposits*. Chapman & Hall, London.

Kohlmann, M., Sowa, H., Reithmayer, K. & Schulz, H. 1994, Structure of a $Y_{1-x}(Gd,Dy,Er)_xPO_4 \cdot 2H_2O$ microcrystal using synchrotron radiation. *Acta Crystallographica*, C50: 1651-1652.

Lucas, S., Champion, E., Bregiroux, D., Bernache-Assolant, D. & Audubert, F. 2004, Rare earth phosphate powders $RePO_4 \cdot nH_2O$ (Re = La, Ce or Y)-Part I. Synthesis and characterization. *Journal of Solid State Chemistry*, 177: 1302-1311.

Marincea, Ş., Dumitraş, D.-G. 2003, The occurrence of taranakite in the "dry" Cioclovina Cave (Şureanu Mountains, Romania). *Neues Jahrbuch für Mineralogie, Monatshefte*, 3: 127-144.

Marincea, Ş., Dumitraş, D.-G. 2005, First reported sedimentary occurrence of berlinite ($AlPO_4$) in phosphate-bearing sediments from Cioclovina Cave, Romania - Comment. *American Mineralogist*, 90: 1203-1208.

Marincea, Ş., Dumitraş, D.-G & Gibert, R. 2002, Tinsleyite in the "dry" Cioclovina Cave (Şureanu Mountains, Romania) the second occurrence. *European Journal of Mineralogy*, 14: 157-164.

Martini, J.E.J. 1994a, Two new minerals originated from bat guano combustion in Arnhem Cave, Namibia. *Bulletin of the South African Speleological Association*, 33: 66-69.

Martini, J.E.J. 1994b, The combustion of bat guano – a poorly known phenomenon. *Bulletin of the South African Speleological Association*, 33: 70-72.

Martini, J.E.J. 1997, Pyrocoproite ($Mg(K,Na)_2P_2O_7$, monoclinic), a new mineral from Arnhem Cave (Namibia), derived from bat guano combustion. In *Proceedings of the 12th International Congress of Speleology* (Jeannin, P.-Y., Ed.), La Chaux-de-Fonds, Switzerland, 1: 223-225.

McConnell, D. 1937, The substitution of SiO_4^- and SO_4^- groups for PO_4^- groups in the apatite structure; ellestadite, the end-member. *American Mineralogist*, 22: 977-986.

Millero, F.J. 1992, Stability constants for the formation of rare earth-inorganic complexes as a function of ionic strength. *Geochimica et Cosmochimica Acta*, 56: 3123-3132.

Moore, P.B., Kampf, A.R. & Araki, T. 1975, Foggite, $Ca(H_2O)_2[CaAl_2(OH)_4(PO_4)_2]$: its atomic arrangement and relationship to calcium Tschermak's pyroxene. *American Mineralogist*, 60: 965-971.

Muraoka, Y., Kihara, K. 1997, The temperature dependence of the crystal structure of berlinite, a quartz-type form of $AlPO_4$. *Physics and Chemistry of Minerals*, 24: 243-253.

Nonius, B.V. 1999, "Collect". Data collection software.

Oakley, K.P. 1954, Evidence of fire in South African cave deposits. *Nature*, 174: 261-262.

Olariu, A., Hellborg, R., Stenström, K., Skog, G., Faarinen, M., Persson, P., Erlandsson, B. & Alexandrescu, E. 2002, Dating of some Romanian fossil bones by combined nuclear methods. *Journal of Radioanalytical and Nuclear Chemistry*, 253 (2): 307–311.

Onac, B.P. 2003, Checklist of the Romanian cave minerals. *Theoretical and Applied Karstology*, 16: 83-89.

Onac, B.P. 2005, Minerals. In *Encyclopedia of Caves* (Culver, D.C, White, W.B., Eds.), Elsevier/Academic Press, Amsterdam, p. 371-378.

Onac, B.P., Effenberger, H. 2007, Re-examination of berlinite ($AlPO_4$) from Cioclovina Cave, Romania. *American Mineralogist* (in press).

Onac, B.P., White, W.B. 2003, First reported sedimentary occurrence of berlinite ($AlPO_4$) in phosphate-bearing sediments from Cioclovina Cave, Romania. *American Mineralogist*, 88: 1395-1397.

Onac, B.P., Breban, R., Kearns, J. & Tămaş, T. 2002, Unusual minerals related to phosphate deposits in Cioclovina Cave, Şureanu Mts. (Romania). *Theoretical and Applied Karstology*, 15: 27-34.

Onac, B.P., Effenberger, H., Ettinger, K. & Cîntă-Pânzaru, S. 2006, Hydroxylellestadite from Cioclovina Cave (Romania): Microanalytical, structural, and vibrational spectroscopy data. *American Mineralogist*, 91: 1927-1931.

Onac, B.P., Ettinger, K., Kearns, J. & Balasz, I.I. 2005, A modern, guano-related occurrence of foggite, $CaAl(PO_4)(OH)_2 \cdot H_2O$ and churchite-(Y), $YPO_4 \cdot 2H_2O$ in Cioclovina Cave, Romania. *Mineralogy and Petrology*, 85: 291-302.

Otwinowski, Z., Minor, W. 1997, Processing of X-ray diffraction data collected in oscillation mode. In *Methods in Enzymology* (Carter Jr., C.V., Sweet, R.M., Eds.), v. 276, Macromolecular Crystallography A, Academic Press, New York, p. 307-326.

Păunescu, A. 2001, *The Paleolithic and Mesolithic from the Transylvanian basin*. Ed. AGIR, Bucureşti, 574 p. (in Romanian)

Petruševski, V., Šoptrajanov, B. 1984, Infrared spectra of the dehydrates of calcium selenate and yttrium phosphate – comparison with the spectrum of gypsum. *Journal of Molecular Structure*, 115: 343-346.

Popović, L., de Waal, D. & Boeyens, J.C.A. 2005, Correlation between Raman wavenumbers and P-O bond lengths in crystalline inorganic phosphates. *Journal of Raman Spectroscopy*, 36: 2-11.

Roska, M. 1925, Recherches sur le Paleolithic en Transylvania. *Buletinul Societăţii de Ştiinţe Cluj,* Tome II (4): 183-184.

Santos, R.V., Clayton, R.N. 1995, The carbonate content in high temperature apatite: An analytical method applied to apatite from the Jacupiranga alkaline complex. *American Mineralogist*, 80: 336-344.

Sejkora, J., Houzar, S. & Šrein, V. 1999, Cl-rich hydroxyl-ellestadite from Zastávka near Brno. *Acta Musei Moraviae, Scientiae Geologicae*, 84: 49-59 (in Czech with English abstract).

Sheldrick, G.M. 1997, SHELXL-97, a program for crystal structure refinement. University of Göttingen, Germany.

Simionescu, I. 1941, The *Ursus spelaeus* from the Cioclovina Cave. *Analele Academiei Române, Memoriile Secţiunii Ştiinţifice,* seria III, XVII (7): 383-402 (in Romanian).

Socrates, G. 2001, *Infrared and Raman Characteristic Group Frequencies, Tables and Charts*. Wiley, Chichester.

Sowa, H., Macavei, J. & Schulz, H. 1990, The crystal structure of berlinite $AlPO_4$ at high pressure. *Zeistschrift für Kristallographie*, 192: 119-136.

Stillă, A. 1981, Géologie de la region de Haţeg-Cioclovina-Pui-Băniţa (Carpates Meridionales. *Anuarul Institutului de Geologie şi Geofizică*, 66: 91-179.

Urbani, F. 1996, Venezuelan cave minerals, a review. *Boletín de la Sociedad Venezolana de Espeleologia*, 30: 1-13.

Yvon, K., Jeitschko, W. & Parthé, E. 1977, LAZY PULVERIX, a computer program for calculating X-ray and neutron powder patterns. *Journal of Applied Crystallography*, 10: 73-74.